REPORT

PHOTOSYNTHESIS

Photochemistry beyond the red limit in chlorophyll f-containing photosystems

Dennis J. Nürnberg[1]*, Jennifer Morton[2], Stefano Santabarbara[3], Alison Telfer[1], Pierre Joliot[4], Laura A. Antonaru[1], Alexander V. Ruban[5], Tanai Cardona[1], Elmars Krausz[3], Alain Boussac[6], Andrea Fantuzzi[1]*, A. William Rutherford[1]*

Photosystems I and II convert solar energy into the chemical energy that powers life. Chlorophyll a photochemistry, using red light (680 to 700 nm), is near universal and is considered to define the energy "red limit" of oxygenic photosynthesis. We present biophysical studies on the photosystems from a cyanobacterium grown in far-red light (750 nm). The few long-wavelength chlorophylls present are well resolved from each other and from the majority pigment, chlorophyll a. Charge separation in photosystem I and II uses chlorophyll f at 745 nm and chlorophyll f (or d) at 727 nm, respectively. Each photosystem has a few even longer-wavelength chlorophylls f that collect light and pass excitation energy uphill to the photochemically active pigments. These photosystems function beyond the red limit using far-red pigments in only a few key positions.

Oxygenic photosynthesis uses chlorophyll a (chl a) to convert visible light into chemical energy. The photochemically active pigments of the two photosystems, photosystem I (PSI) and photosystem II (PSII), at 700 nm and 680 nm, respectively, represent the energy available for photochemistry (*1*–*3*) (see supplementary text S1). This was considered the "red limit" (*4*), the minimum energy required for oxygenic photosynthesis, until it was found that a cyanobacterium, *Acaryochloris*, extends this limit by using chl d, a pigment absorbing at a wavelength 40 nm longer than chl a (*5*, *6*). *Acaryochloris* photosystems are dominated (~97%) by chl d with one or two chl a located in key positions (*6*, *7*). More recently, chl f, the longest-wavelength chlorophyll known, was discovered (*6*, *8*, *9*). Chl f exists as a minority pigment in photosystems that contain ~90% chl a. Chl f is generally assumed to play a purely light-harvesting role, needing heat in the environment, the product of the Boltzmann constant and the temperature (k_BT), for uphill excitation transfer to chl a for photochemistry to occur (*5*, *6*, *10*–*13*) [see, however, (*14*)]. Thus, the presence of chl f in these photosystems was not considered an extension of the photochemical red limit. Here, we report data that change that view, showing that long-wavelength chlorophylls perform the photochemistry in both photosystems.

Chroococcidiopsis thermalis, a widely spread extremophile cyanobacterium, when grown under 750-nm far-red light (FRL), contains ~90% chl a, ~10% chl f and <1% chl d. The absorption and fluorescence spectra of the cells were shifted to longer wavelengths with a new absorption peak at 709 nm (Fig. 1A) and 80-K fluorescence at 740, 753, and 820 nm, suggesting changes in both photosystems (Fig. 1B) [see (*10*, *15*)]. These data and decay-associated fluorescence (fig. S1) indicate that the FRL chlorophylls are the dominant terminal emitters and are present in essentially all the photosystems [see also (*9*, *10*)]. The wavelength dependence of PSI and PSII activity (action spectra) in FRL cells were red-shifted (Fig. 1C), with new peaks at 745 nm for PSI and 715 nm for PSII. The action spectra correspond well to the absorption spectra of the isolated photosystems (Fig. 1C). $P_{700}^{\bullet+}$ formation with far-red light was more efficient in FRL cells (Fig. 1D, right). Primary quinone (Q_A) reduction under far-red excitation in white-light (WL) cells was slow and incomplete, but in FRL cells it was very rapid, faster than in WL cells with visible excitation (Fig. 1D, lower middle). O_2 evolution under far-red light reached the same level as seen under visible light in WL cells (see supplementary text S2).

Thermoluminescence (TL) from $S_2Q_B^{\bullet-}$ (Fig. 2A) and $S_2Q_A^{\bullet-}$ (fig. S2A) (*16*) in FRL thylakoids is enhanced by a factor of >25 compared with WL thylakoids. TL arises from repopulation of the excited state of the primary donor chlorophyll, $^*Chl_{D1}$, by charge recombination, which then emits at the same wavelength as the prompt fluorescence (*17*). The enhancement in TL intensity in FRL PSII indicates a decrease in the energy gap between the precursor charge pair and the luminescent excited-state chlorophyll (*17*), consistent with a lower-energy, longer-wavelength primary donor/emitter (supplementary text S3). Recombination takes place at temperatures close to those seen in the WL PSII, and the flash-number dependence is nearly identical to that seen in WL PSII, indicating no obvious change in the yields of charge separation and stabilization (fig. S2B).

PSII activity, measured as the rates of Q_A reduction at 293 (Fig. 2B, inset) and 77 K (Fig. 2B) and as the rate of β-carotene cation radical formation at 15 K (*18*, *19*), were comparable with red and far-red excitation (Fig. 2C and fig. S3). A purely antenna role for chl f (*5*, *6*, *10*–*13*) would require that heat (k_BT) drives the excitation from the shortest-wavelength chl f (~720 nm) uphill to P_{680}, the chl a primary donor. The k_BT at room temperature (293 K) is 26 meV and too small to cover the ~100 meV energy gap between 720 and 680 nm. Although some overlap of the absorption bands could allow this process to occur inefficiently at 293 K, thermally induced excitation transfer will become vanishingly weak at 77 K (k_BT = 6.6 meV) and 15 K (k_BT = 1.3 meV) (supplementary text S4). The matching rates for PSII photochemistry with red and far-red excitation at cryogenic temperatures indicate that a FRL chlorophyll is involved in primary charge separation.

When the $Pheo_{D1}^{\bullet-}$ is trapped by illumination in the presence of a reductant (*20*, *21*) the light-minus-dark difference spectrum exhibits the expected bleaches at ~546 and ~680 nm (Fig. 2D) due to the disappearance of the $Pheo_{D1}$ Q_y and Q_x absorptions. In WL PSII, the charge on $Pheo_{D1}^{\bullet-}$ induces a blue shift of the Chl_{D1} Q_y absorption at ~680 nm. This electrochromic shift dominates the difference spectrum (*20*, *21*) but is notably absent in the FRL PSII (Fig. 2D). Instead, a marked blue shift at ~720 nm is seen. This indicates that Chl_{D1} is a long-wavelength chlorophyll in FRL PSII. The smaller blue-shift feature at ~669 nm is attributed to P_{D1}/P_{D2}.

When $Q_A^{\bullet-}$ is trapped by illumination at 77 K (Fig. 2E), the charge created on $Q_A^{\bullet-}$ is known to induce a blue shift of the Q_y band of Chl_{D1} (*21*). In FRL PSII, the Chl_{D1} blue shift typically seen near ~680 nm (*21*) is replaced by one at ~727 nm. This indicates that Chl_{D1} is replaced by a FRL chlorophyll (Fig. 2F). The absence of the Chl_{D1} band shift at 680 nm allows a 685-nm red shift to become evident. This corresponds to the expected (but not previously visible) $Q_A^{\bullet-}$-induced shift of the $Pheo_{D1}$ Q_y excitation (supplementary text S2).

High-performance liquid chromatography (HPLC) indicated that the isolated PSII contained 2 pheo a, 4 chl f, 1 chl d, and 30 chl a per center, based on the 35 chl per PSII (*22*) (fig. S5A). The 77-K absorption spectrum (Fig. 2E) shows four peaks above 700 nm. The 710-nm

[1]Department of Life Sciences, Imperial College, London SW7 2AZ, UK. [2]Research School of Chemistry, ANU, Canberra, Australia. [3]Istituto di Biofisica, Consiglio Nazionale delle Ricerche, via Celoria 26, 20133 Milano, Italy. [4]Institut de Biologie Physico-Chimique, Unité Mixte de Recherche 7141 Centre National de la Recherche Scientifique-Université Pierre et Marie Curie, 13 Rue Pierre et Marie Curie, 75005 Paris, France. [5]School of Biological and Chemical Sciences, Queen Mary University of London, London E1 4NS, UK. [6]Institut de Biologie Intégrative de la Cellule, UMR 9198, Bât 532, CEA Saclay, 91191 Gif-sur-Yvette, France.
***Corresponding author. Email: a.rutherford@imperial.ac.uk (A.W.R.); d.nurnberg@imperial.ac.uk (D.J.N.); a.fantuzzi@imperial.ac.uk (A.F.)**

band is attributed to red-shifted allophycocyanins (*9*, *23*), based on its wavelength, variable amplitude in different preparations, and absence of magnetic circular dichroism (MCD) (fig. S6). The 1.8-K absorption and MCD spectra were fitted with ~5 FRL chlorophylls at 721, 727, 734, 737, and 749 nm (fig. S7).

Intrinsically, chl d absorbs at shorter wavelengths than chl f; thus, it is the most obvious choice for the 721-nm pigment. This pigment could be a linker between the primary donor at 727 nm and the shorter-wavelength antenna (supplementary text S5). Given the small wavelength difference, we need to consider the possibility that chl d is the primary donor, Chl_{D1}. The wavelength (727 nm) of the primary donor is similar to the chl d (725 nm) in this location in *Acaryochloris* (*7*, *24*).

The conserved amino acid changes near Chl_{D1} (figs. S8 and S9) suggest specific H bonding to a formyl group on either the C2 (chl f) or C3 (chl d) position of Chl_{D1}. This provides further evidence that Chl_{D1} in FRL PSII is a long-wavelength chlorophyll but does not discriminate between chl d and chl f (fig. S8). The three remaining long-wavelength chlorophylls appear to be tuned to span the energy gap from 749 nm up to the photochemically active chlorophyll at 727 nm, with gaps of 10 to 12 nm (23 to 26 meV), appropriate to the value of k_BT at ambient temperatures (~26 meV) (see supplementary text S5 and table S1 for other pigment assignments).

It seems likely that P_{D1}, which bears the key long-lived chlorophyll cation radical, remains a chl a. This suggestion is based on (i) the presence of the blue shifts at 669 nm attributed to P_{D1} (Fig. 2, D and E), (ii) structural considerations (figs. S8 and S12), (iii) the precedence of chl a being P_{D1} in *Acaryochloris* (*6*, *7*, *24*), and (iv) conservation of specific chemical properties (e.g. oxidizing power, stability, and reactivity) without the need for major redox and kinetic tuning. Nevertheless, sequence comparisons indicate changes in the environments of cofactors in the redox core, including P_{D1}, likely reflecting the tuning needed to adjust to the presence of the long-wavelength pigment. (see table S2 and figs. S9 and S12 to S14).

When isolated FRL PSI was excited at 15 K using 610-, 730-, and 750-nm light, comparable photochemistry was seen (Fig. 3A and fig. S15), indicating that the chlorophyll absorbing at ~750 nm is involved in charge separation. In WL PSI, 750-nm excitation resulted in the expected low-quantum-yield photochemistry (Fig. 3A) due to weak optical charge-transfer absorption at 750 nm (supplementary text S4).

Light-minus-dark difference spectra at 293 K in FRL and WL thylakoids are similar to those obtained at 77 and 1.8 K from isolated FRL and WL PSI, except for thermal broadening at higher temperatures (Fig. 3B and fig. S16). The

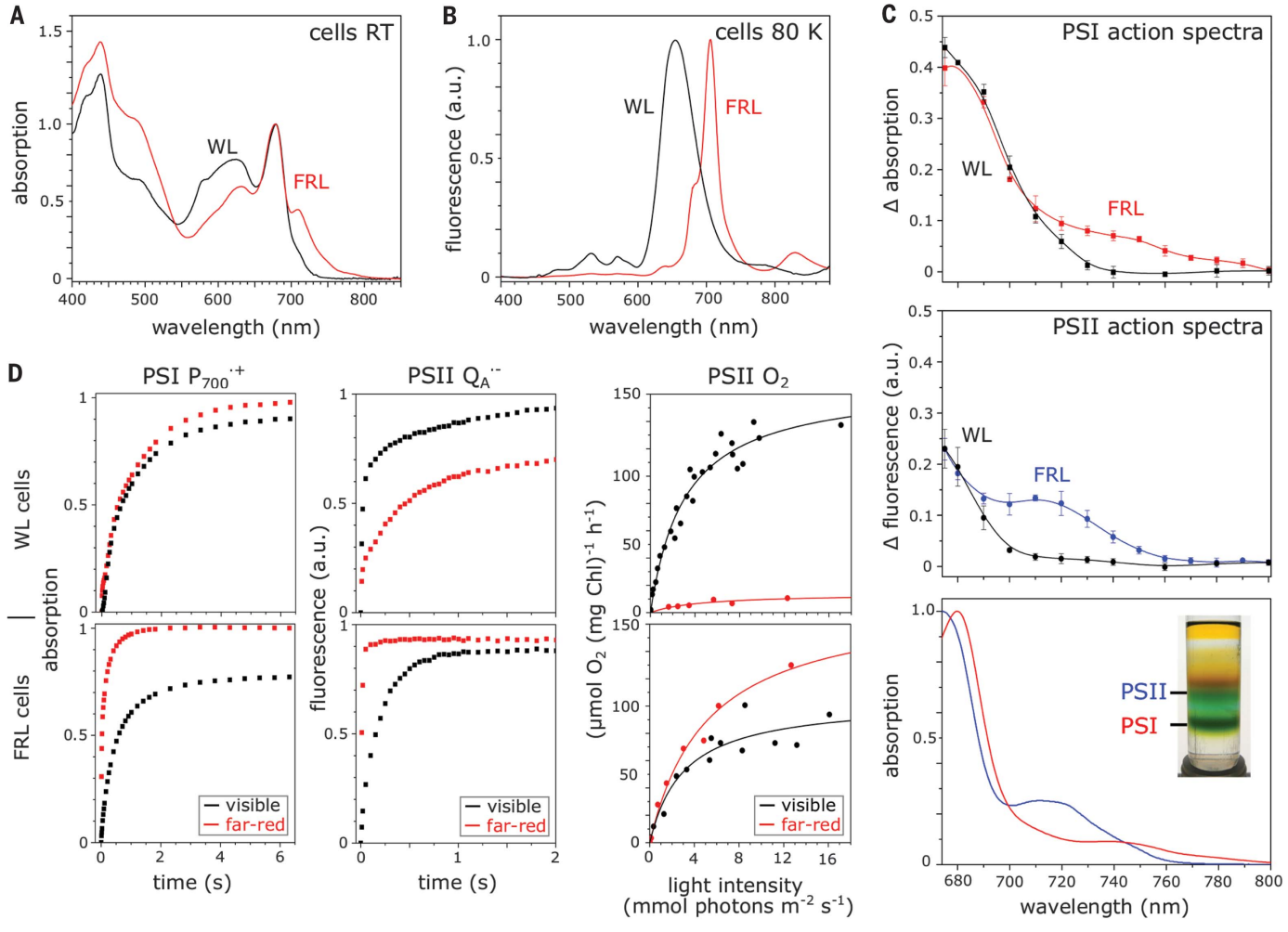

Fig. 1. Changes in the pigments and activities of the photosystems from *C. thermalis* cells grown in 750-nm light. (**A**) Absorption spectra and (**B**) 80 K fluorescence spectra of WL and FRL cells. (**C**) Action spectra for PSI ($P_{700}^{\cdot+}$ at 430 nm, 50 μs after the flash) (top) and PSII ($Q_A^{\cdot-}$ +DCMU, measured as fluorescence) (middle) in FRL cells (red and blue, respectively) compared to WL cells (black). Bottom panel: absorption spectra from isolated PSI (red) and PSII (blue); inset sucrose gradient separating the photosystems. (**D**) Photosystem activities measured in WL (top) and FRL cells using visible (black) and far-red (red points) excitation. Left: PSI activity ($P_{700}^{\cdot+}$ at 705 nm 50 μs after the flash). Middle: PSII activity ($Q_A^{\cdot-}$ as in C). Right: O_2 evolution as a function of light intensity. See materials and methods for details.

main bleach is at ~704 nm with an absorption increase at 692 nm, indicating that the cation is located on the P_AP_B chlorophyll a/a' pair, $P_{700}^{\bullet+}$, as seen in WL PSI. The rest of the spectrum shows marked differences: the sharp trough at 684 nm, the peak at 674 nm (680 nm at 77 K), and the trough at 656 nm (~660 nm at 77 K), all of which are present in WL PSI (Fig. 3B and fig. S16) but are absent in FRL PSI. Instead, several changes appear at >700 nm (Fig. 3B). These changes can be attributed to the replacement of chl a band shifts in WL PSI with long-wavelength chlorophyll band shifts in FRL PSI. The band shifts at >700 nm are better resolved at 77 and 1.8 K and show a broad blue-shift feature (or two overlapping blue shifts) at ~745 nm, a sharp red shift at 756 nm, and a weak blue shift at 800 nm. In addition, there is a red shift at ~684 nm, which is likely present in WL PSI but now resolved in the FRL PSI.

HPLC shows that FRL PSI contains 0 pheo, 7 to 8 chl f, 0 chl d, and ~88 to 89 chl a (fig. S5B), assuming 96 chl per PSI (*25*). The 1.8 K absorption and MCD spectra at >700 nm (fig. S17) can be fitted as follows: 1 chl f at 736 nm, 3 chl f at ~745 nm, 1 chl f at 756 nm, 1 chl f at ~763 nm, and ~2 chl f at ~800 nm (fig. S18). In addition, a chlorophyll feature at 709 nm is suggested to be a long-wavelength PSI chl a.

Based on the crystal structure (*25*), the difference spectra (Fig. 3B and fig. S16), the low-temperature photochemistry (Fig. 3A and fig. S15), and structural arguments (figs. S8 and S19), the following model emerges for the FRL PSI redox cofactors: (i) P_A and P_B remain chl a/chl a′ and bear the P_{700} cation. (ii) A_{0A} and A_{0B}, the primary acceptors (*1*, *26*), remain chl a, because the redox properties of chl f (*13*) make it unsuitable for a low potential role. This fits with the assignment of the ~684-nm red shift to A_0 (Fig. 3B) [see (*26*)] and with A_0 being chl a in *Acaryochloris* (*24*). (iii) One or both of the primary donors, A_{1A} and A_{1B} (*27*), are chl f in FRL PSI, absorbing at ~745 nm. The difference spectra seem to arise from overlapping blue shifts at this wavelength, replacing the dominant ~684-nm blue shift in the WL PSI. A_{1A} and A_{1B} are the only redox-active chlorophylls oriented to allow a blue shift. Possible locations of the six chl f antenna are discussed in the supplementary materials (supplementary text S6).

The far-red photosystems studied here represent a third paradigm for oxygenic photosynthesis (supplementary text S1). The first is the canonical type that use chl a for both charge separation and antenna absorption. The second is that of *Acaryochloris*, where chl d replaces all chl a for both photochemistry and light harvesting, with the exception of chl a being retained in two key redox roles: P_{D1}, where $P_{D1}^{\bullet+}$ is the principle oxidant of PSII, and A_0, where $A_0^{\bullet-}$ is the principle reductant in PSI. The new paradigm maintains chl a in nearly all positions except for a small number of chl f molecules (plus one chl d in PSII). These long-wavelength chlorophylls act as (i) the primary electron donors in both photosystems, (ii) linkers to shorter-wavelength antenna pigments, and (iii) a small, longer-wavelength antenna system. The far-red photosystems provide well-resolved absorption spectra at long wavelengths due to the decreased spectral overlap, which allows more definitive assignments and analyses.

Chl f can absorb at >760 nm, yet the wavelength used to drive photochemistry in the FRL PSII is ~727 nm (fig. S20). This wavelength is similar to that of the chl d primary donor (Chl_{D1}) in *Acaryochloris* PSII (*6*, *7*, *24*). Thus, both of the known cases of PSII functioning "beyond the red limit" use primary donors with similar energies. This may represent a "second red limit" for PSII, one that applies in the stable, deep-shade environments where far-red photosynthesis occurs in nature. The ~110 meV of energy sacrificed by the shift from ~680 to 727 nm may correspond to the energy "headroom" needed by PSII to mitigate the photodamage caused by variable light intensities (*3*, *28*, *29*). This potential disadvantage may explain why oxygenic photosynthesis using far-red light is restricted to rare, deep-shade

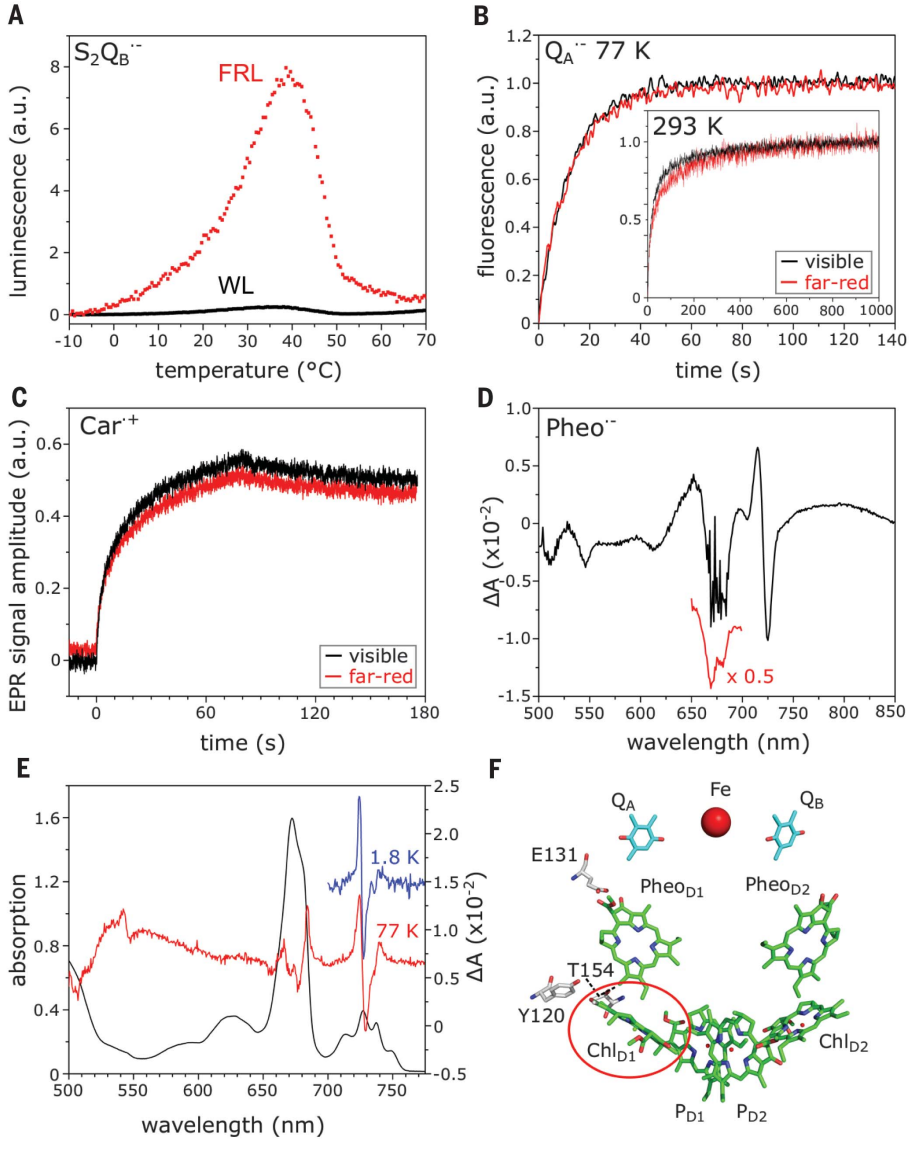

Fig. 2. FRL PSII photochemistry. (**A**) $S_2Q_B^{\bullet-}$ thermoluminescence in WL and FRL thylakoids from *C. thermalis*. (**B**) Kinetics of Q_A reduction in FRL thylakoids (measured as fluorescence) at 77 K (inset at 293 K). Samples were excited using visible (600-nm) and far-red (710-nm) light. (**C**) Kinetics of β-carotene cation radical formation in isolated FRL PSII at 15 K illuminated with visible (610-nm) and far-red (730-nm) light. (**D**) Light-minus-dark visible/near-IR spectrum at 293 K upon $Pheo_{D1}^{\bullet-}$ formation in isolated FRL PSII. The 650- to 700-nm region is saturated in the main spectrum (black), the red inset is a 2x-diluted sample. (**E**) 77-K absorption spectrum of isolated FRL PSII (black) with the 77-K (red) and 1.8-K (blue) 725-nm illuminated-minus-dark difference spectra. (**F**) Cofactors in PSII showing Chl_{D1} as a FRL chlorophyll (circled) and potential H-bonding amino acids, based on the crystal structure PDB 3WU2 (*22*).

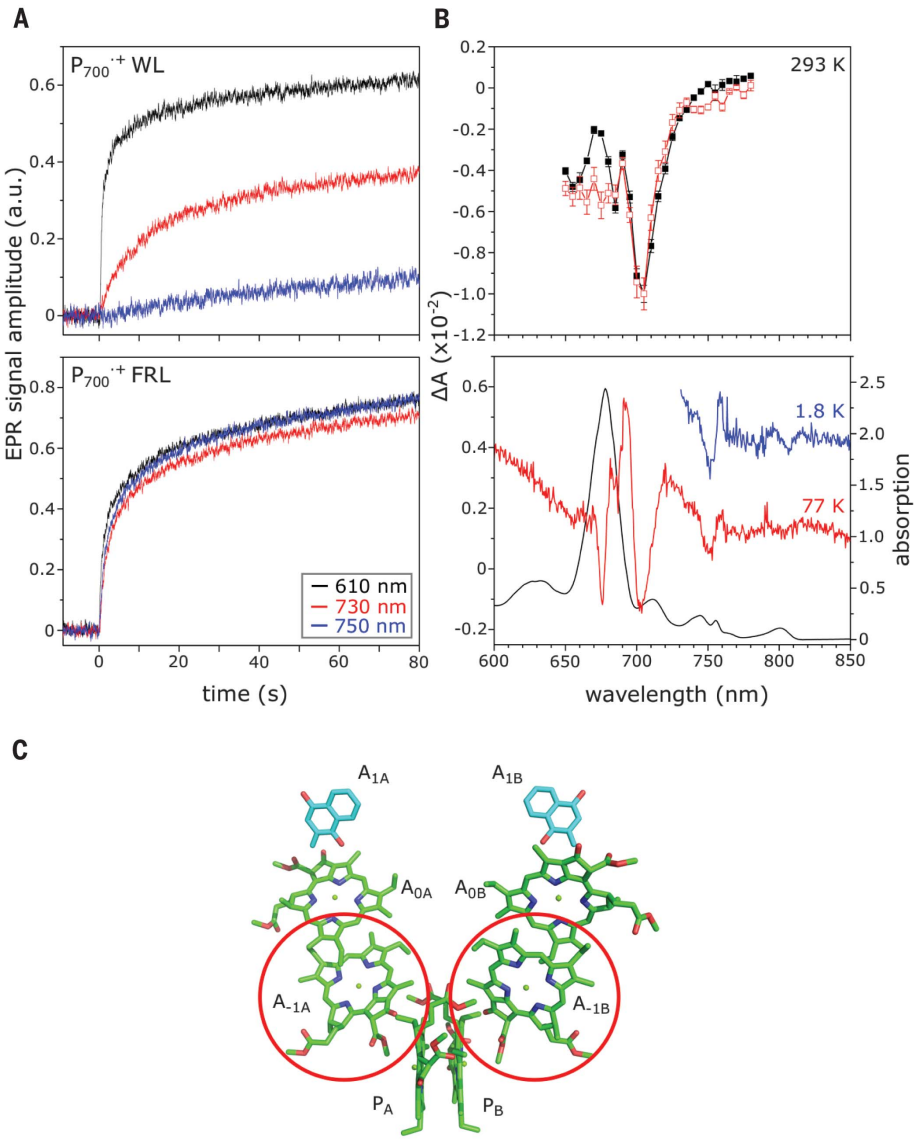

Fig. 3. FRL PSI photochemistry. (**A**) 15-K photo-accumulation of $P_{700}^{\bullet+}$ monitored by EPR using visible and far-red light in (top) isolated FRL PSI and (bottom) isolated WL PSI. (**B**) (Top) Flash-induced $P_{700}^{\bullet+}$ 293-K absorption difference spectrum using FRL and WL thylakoids. (Bottom) $P_{700}^{\bullet+}$ 77-K (red) and 1.8-K (blue) difference spectra and 1.8-K absorption spectrum (black) of isolated FRL PSI. (**C**) FRL PSI model (PDB 1JB0) (*25*). Red circles show the proposed locations of chl f, with other positions as chl a (see the text).

environments, rich in far-red light (supplementary text S7).

REFERENCES AND NOTES

1. J. H. Golbeck, Ed., *Photosystem I. The Light-Driven Plastocyanin: Ferredoxin Oxidoreductase* (Springer Netherlands, 2006).
2. H. Dau, I. Zaharieva, *Acc. Chem. Res.* **42**, 1861–1870 (2009).
3. A. W. Rutherford, A. Osyczka, F. Rappaport, *FEBS Lett.* **586**, 603–616 (2012).
4. L. O. Björn, G. C. Papageorgiou, R. E. Blankenship, Govindjee, *Photosynth. Res.* **99**, 85–98 (2009).
5. P. Loughlin, Y. Lin, M. Chen, *Photosynth. Res.* **116**, 277–293 (2013).
6. H. Miyashita *et al.*, *J. Phys. Chem. Biophys.* **4**, 149 (2014).
7. T. Renger, E. Schlodder, *J. Phys. Chem. B* **112**, 7351–7354 (2008).
8. M. Chen *et al.*, *Science* **329**, 1318–1319 (2010).
9. F. Gan *et al.*, *Science* **345**, 1312–1317 (2014).
10. S. Itoh *et al.*, *Plant Cell Physiol.* **56**, 2024–2034 (2015).
11. S. I. Allakhverdiev *et al.*, *Biochem.* **81**, 201–212 (2016).
12. D. M. Niedzwiedzki, H. Liu, M. Chen, R. E. Blankenship, *Photosynth. Res.* **121**, 25–34 (2014).
13. M. Kobayashi *et al.*, in *Photosynthesis*, Z. Dubinsky, Ed. (InTech, 2013).
14. M. Kaucikas, D. Nürnberg, G. Dorlhiac, A. W. Rutherford, J. J. van Thor, *Biophys. J.* **112**, 234–249 (2017).
15. C. Zhao, F. Gan, G. Shen, D. A. Bryant, *Front. Microbiol.* **6**, 1–13 (2015).
16. A. W. Rutherford, A. R. Crofts, Y. Inoue, *Biochim. Biophys. Acta* **682**, 457–465 (1982).
17. F. Rappaport, J. Lavergne, *Photosynth. Res.* **101**, 205–216 (2009).
18. W. W. I. Adams 3rd, B. Demmig-Adams, K. Winter, U. Schreiber, *Planta* **180**, 166–174 (1990).
19. J. Hanley, Y. Deligiannakis, A. Pascal, P. Faller, A. W. Rutherford, *Biochemistry* **38**, 8189–8195 (1999).
20. V. V. Klimov, A. V. Klevanik, V. A. Shuvalov, A. A. Kransnovsky, *FEBS Lett.* **82**, 183–186 (1977).
21. N. Cox *et al.*, *J. Phys. Chem. B* **113**, 12364–12374 (2009).
22. Y. Umena, K. Kawakami, J.-R. Shen, N. Kamiya, *Nature* **473**, 55–60 (2011).
23. Y. Li *et al.*, *Biochim. Biophys. Acta Bioenergetics* **1857**, 107–114 (2016).
24. S. Itoh *et al.*, *Biochemistry* **46**, 12473–12481 (2007).
25. P. Jordan *et al.*, *Nature* **411**, 909–917 (2001).
26. A. Chauvet, N. Dashdorj, J. H. Golbeck, T. W. Johnson, S. Savikhin, *J. Phys. Chem. B* **116**, 3380–3386 (2012).
27. M. G. Müller, C. Slavov, R. Luthra, K. E. Redding, A. R. Holzwarth, *Proc. Natl. Acad. Sci. U.S.A.* **107**, 4123–4128 (2010).
28. C. A. R. Cotton *et al.*, *Front. Bioeng. Biotechnol.* **3**, 36 (2015).
29. G. A. Davis *et al.*, *eLife* **5**, 1–27 (2016).

ACKNOWLEDGMENTS

We gratefully acknowledge our friend and colleague Fabrice Rappaport, who died in January 2016, with whom we worked in the early stages of this project. We thank J. Murray for discussions, B. Nwaobi for technical support, C. Mullineaux for access to a 77-K fluorometer, B. Bailleul and W. Remelli for technical help in obtaining the absorption spectra, J.-M. Ducruet for lending us the thermoluminescence setup, and L. Haigh for her assistance with the HPLC analysis. **Funding:** This work was supported by BBSRC grants BB/L011506/1 and BB/R001383/1, Leverhulme Trust grant RPG-2017-223 and a Wolfson Merit Award from the Royal Society to A.W.R., Australian Research Council grant DP150103137 to E.K., an Imperial College Junior Research Fellowship to T.C. and an ANR-10-INBS-05 (FRISBI) grant to A.B. **Author contributions.** D.J.N. initiated the study, built growth chambers, surveyed, selected and grew the strains. D.J.N., A.F., and A.W.R. conceived of the main experiments, collated results and interpretations, and wrote the article with input, edits, and approval from all authors. D.J.N. with A.T. and A.B. developed and did the isolation of the photosystems. J.M. with E.K. did the low-temperature optical spectroscopy (visible/near IR, CD, MCD, fluorescence). S.S. and D.J.N. did 293 K and 77 K visible/near IR spectroscopy on PSI. D.J.N. and A.T. did the HPLC. A.B. and A.W.R. did the EPR. L.A.A. with D.J.N. did the O_2 evolution. A.F. and D.J.N. did the TL. A.F. did the $Pheo^{\bullet-}$ trapping and wavelength dependence of $Q_A^{\bullet-}$ at 293 and 80 K. P.J. and D.J.N. did the wavelength dependence of PSI and PSII activities in cells. D.J.N. and A.W.R. worked with F. Rappaport to obtain the action spectra with advice from P.J. A.V.R. and D.J.N. did the time-resolved fluorescence studies, and S.S. helped with the interpretation. A.F. and T.C. did the modeling studies. E.K. and D.J.N. did the curve fitting, with input from J.M., S.S., A.F., and A.W.R. **Competing interests:** The authors declare no competing interests. **Data and materials availability:** All data are available in the manuscript or the supplementary material.

SUPPLEMENTARY MATERIALS

www.sciencemag.org/content/360/6394/1210/suppl/DC1
Materials and Methods
Supplementary Text S1 to S7
Figs. S1 to S20
Tables S1 to S3
References (*30*–*92*)
Data S1

22 December 2017; accepted 18 April 2018
10.1126/science.aar8313

Photochemistry beyond the red limit in chlorophyll f–containing photosystems

Dennis J. Nürnberg, Jennifer Morton, Stefano Santabarbara, Alison Telfer, Pierre Joliot, Laura A. Antonaru, Alexander V. Ruban, Tanai Cardona, Elmars Krausz, Alain Boussac, Andrea Fantuzzi and A. William Rutherford

Science **360** (6394), 1210-1213.
DOI: 10.1126/science.aar8313

Lower-energy photons do the work, too

Plants and cyanobacteria use chlorophyll-rich photosystem complexes to convert light energy into chemical energy. Some organisms have developed adaptations to take advantage of longer-wavelength photons. Nürnberg *et al.* studied photosystem complexes from cyanobacteria grown in the presence of far-red light. The authors identified the primary donor chlorophyll as one of a few chlorophyll molecules in the far-red light–adapted enzymes that were chemically altered to shift their absorption spectrum. Kinetic measurements demonstrated that far-red light is capable of directly driving water oxidation, despite having less energy than the red light used by most photosynthetic organisms.
Science, this issue p. 1210